

Application of palynomorphs and palynofacies in Early Cretaceous paleoenvironmental reconstruction; Shushan Basin, Egypt

MAGDY MAHMOUD¹, AMAL TEMRAZ², ABDEL-RAHIM MOAWAD² and MIRAN KHALAF^{3*}

¹ *Geology Department, Faculty of Science, Assiut University, Assiut 71516, Egypt;*
e-mail: magdysm@aun.edu.eg

² *Geology Department, Faculty of Science, South Valley University, Qena 83523, Egypt;*
e-mails: amalatemraz@yahoo.com, abdelrahimoawad@gmail.com

³ *Geology Department, Faculty of Science, Sohag University, Sohag 82524, Egypt;*
e-mails: miran_kha2@science.sohag.edu.eg, miran_kha2@yahoo.com

* Corresponding author

ABSTRACT:

Mahmoud, M., Temraz, A., Moawad, A.-R. and Khalaf, M. 2024. Application of palynomorphs and palynofacies in Early Cretaceous paleoenvironmental reconstruction; Shushan Basin, Egypt. *Acta Geologica Polonica*, **74** (2), e13.

An integration of palynomorph and palynofacies data from the Shushan-1X well is used to infer the paleoenvironmental conditions of the Valanginian to Middle Cenomanian (Cretaceous) section of the western Shushan Basin, northern Egypt. The data obtained contribute significantly to the depositional history of the basin. The low diversity of dinoflagellate cyst assemblages, along with the dominance of land-derived spores and pollen, suggest restricted (marginal) marine environments, in contrast to their coeval representatives from the Tethyan Realm. Open marine (inner shelf) environments developed at a few horizons in the Dahab and Bahariya formations, partly contemporary with the global Aptian and Cenomanian eustatic cycles. These environments were relatively more offshore than those described in the eastern and southeastern parts of the basin. The study of total palynological organic matter (TPOM) has contributed largely to these established environmental settings. It has also allowed the recognition of redox (suboxic to anoxic) conditions and the impact of a large magnitude of terrigenous influence.

Key words: Cretaceous; Paleoenvironment; Palynomorphs; Palynofacies; Egypt.

INTRODUCTION

Palynological studies during the last three decades have contributed to the biostratigraphy and paleoecology of Cretaceous sediments in the subsurface of northern Egypt (e.g., Schrank and Mahmoud 1998; Mahmoud *et al.* 2017, 2019; El Atfy *et al.* 2023). A preliminary palynological study in the Lower Cretaceous interval, penetrated by the presently investigated Shushan-1X well (Text-fig. 1), was conducted more than thirty years ago (Moawad 1990);

incomplete information on the biostratigraphic and paleoenvironmental significance of terrestrial pollen and spores, along with a few marine dinoflagellate cysts, was presented. Recently, Mahmoud *et al.* (2023) carried out a detailed palynostratigraphic analysis on the Valanginian to Cenomanian interval of the same well and proposed a high-resolution biostratigraphic scheme.

We aim to reconstruct the paleoenvironment using a high-resolution set of samples. Inferences of redox conditions, terrestrial/freshwater influx, prox-





Text-fig. 1. Map showing the location of the investigated Shushan-1X well and positions of the main Mesozoic basins in the Western Desert of Egypt (modified after Shalaby *et al.* 2012).

imity of deposition sites to land, vegetation cover on ancient landscapes and paleoclimate were targeted. We incorporated previously established data to offer insights into the regional paleoenvironmental setting of the basin under study.

GEOLOGICAL SETTING

Fragmentation of the Gondwana continent resulted in the formation of several hydrocarbon-bearing rift basins and the opening of the southern Neo-Tethys that were developed during the Mesozoic in the north of Egypt. These basins are often aligned in a series of E-W, NE-SW and ENE-WSW-oriented half-grabens (e.g., Guiraud *et al.* 2001). The northern Western Desert has a featureless surface, despite its intricate underlying geology. This northern segment of the African Platform is composed of a thick sedimentary Cambrian to Recent succession that gradually slopes seaward. The Shushan Basin probably formed during the Permian-Triassic as a rift basin filled with continental and fluvio-lacustrine sediments. A regional uplift separated this basin into smaller basins not earlier than in the Late Cretaceous (Meshref 1996). The Shushan Basin is one of the main hydrocarbon-producing regions, mainly from the Middle Jurassic Khatatba Formation, the Lower Cretaceous Alam El-Bueib and Alamein formations, and the Upper Cretaceous Abu Roash Formation (e.g., Metwalli and Pigott 2005). The depositional environments varied considerably in the northern part of the Western Desert from the north to

the south. In the north, shallow marine clastics with carbonate intercalations accumulated, whereas continental deposits predominated in the south. These variations reflected local tectonics and/or the ancient paleogeography of the basins (see Hantar 1990; Mahmoud *et al.* 1999, 2017, 2019; El-Soughier *et al.* 2010). Mahmoud *et al.* (2019) suggested a relatively offshore distal setting in the east of the basin, where no hiatuses were detected and the dinoflagellate cysts association contains many open marine forms, and much shallower western and southeastern margins. Mahmoud *et al.* (2019, p. 32) stated that “a palynostratigraphic correlation of monotonous rock units is not only helpful in the detection of lateral continuity of problematic formations, and in tracing their lateral facies change, but also useful in revealing the general paleoceanographic conditions, and in identifying confidently the unrecognizable hiatus”. They suggested also that local paleogeography or uplift were superimposed leading to the missing of the uppermost Alam El-Bueib Formation in the east and the lower Kharita Formation in the southeast.

LITHOSTRATIGRAPHY

The Valanginian to Cenomanian section in the northern Western Desert includes the Alam El-Bueib, Alamein, Dahab, Kharita and Bahariya formations. This sequence consists of sandstones, which grade vertically to siltstones and shales, with limestone intercalations at certain levels (Hantar 1990). These

five formations are briefly described below, from base to top. A revision of the palynological ages of these rock units in the Shushan-1X well was recently established by Mahmoud *et al.* (2023).

Alam El-Bueib Formation (Valanginian to Lower–Middle Aptian)

Norton (1967) first identified this rock unit as part of the Burg El Arab Formation (Barremian to Aptian); then it was formally described in the rank of a formation by Ghorab *et al.* (1971). Its type locality occurs in the Alam El-Bueib-1 well at the depth of 3,927 to 4,297 m. Shale beds occur at the base of the formation, with occasional limestones on top. The formation is regarded as having been deposited in a shallow marine environment with more continental influence towards the south (Hantar 1990; Kerdany and Cherif 1990). Omran *et al.* (1990) and Khalaf (2014) suggested regressive marine conditions (deltaic to inner shelf) for this unit.

Alamein Formation (Lower–Middle to Upper Aptian)

The formation is made up of hard, dense, micro-crystalline dolostones that contain some shale, silty shale and very fine sandstone intercalations (Ghorab *et al.* 1971). The type section is in the Alamein-1 well, in the depth interval from 2,489 to 2,573 m. The formation conformably overlies the Alam El-Bueib Formation and underlies, in places, the Dahab Formation. The Alamein Formation accumulated in shallow marine to deltaic environments (e.g., Kerdany and Cherif 1990; Mahmoud *et al.* 2019).

Dahab Formation (Upper Aptian)

The formation consists mainly of sandstones and shale interbeds. Sandstones are fine- to very fine-grained with calcite cement (Norton 1967). The Dahab Formation overlies the Alamein Formation and underlies the Kharita Formation conformably. Its type section occurs between 3,180 to 3,345 m in the Dahab-1 well, northern Western Desert. The formation reveals a shallow (restricted) marine character (Mahmoud and Moawad 1999).

Kharita Formation (Albian)

The Kharita Formation consists mainly of sandstones with fining upward sequences. Shale and thin limestone beds are sporadically interbedded with

sandstones. Thicker sandstones with shale intercalations occur in the lower part of this unit. Elsewhere, the formation overlies unconformably the Alamein Formation but it overlies the Dahab Formation conformably in the presently investigated well. Its type section is between 2,501 and 2,890 m in the Kharita-1 well (Ghorab *et al.* 1971). The Kharita Formation records a regressive shallow marine high-energy environment (Omran *et al.* 1990).

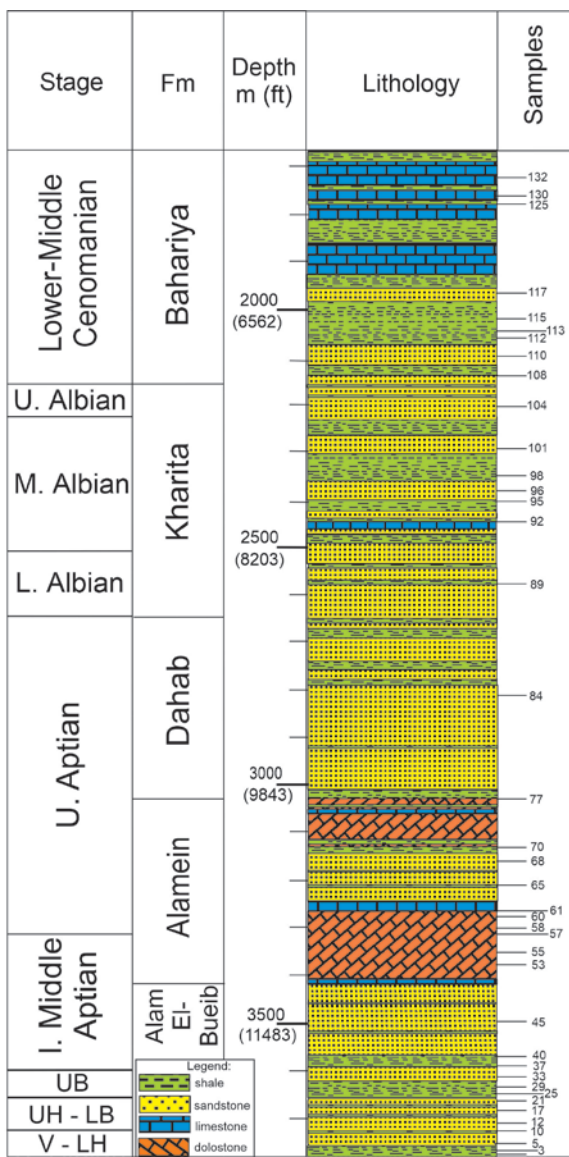
Bahariya Formation (Lower to Middle Cenomanian)

The formation (Norton 1967) covers large areas in the subsurface of the Western Desert and rests, conformably and unconformably, on the Kharita Formation. It is made up of sandstones, siltstones and limestones, alternating with variegated shales; the latter are calcareous and silty. This unit is believed to have been deposited in a fluvio-marine environment. For more paleoenvironmental information, refer to El Beialy *et al.* (2010) and El Atfy *et al.* (2023).

MATERIAL AND METHODS

A comprehensive set of 135 ditch-cutting siltstone samples were collected from the Valanginian to Cenomanian interval of the Shushan-IX well (Text-fig. 2). Samples were processed according to standard palynological procedures (HCl, HF and HCl again, washing and sieving through 10–15 µm nylon sieves). Ultrasonic treatment and oxidation were avoided due to their destructive impact on the palynological organic matter (POM). Then, mild ultrasonic treatment for only a part of the processed residue was performed to concentrate those palynomorphs necessary for the taxonomic study of palynomorphs that are commonly masked by the POM, mainly by the amorphous organic matter (AOM).

For semi-quantitative purposes, three dataset counts were established to estimate the relative abundances of the palynofacies components. The first dataset of at least 500 particles was established to account for the relative abundances of the total palynological organic matter (TPOM), such as AOM, brown wood, opaque phytoclasts and palynomorphs in all samples of the Shushan-1X well. Afterwards, the second dataset was created by establishing up to, at least, 500 particles, without the palynomorphs, to calculate the relative percentages of palynodebris. Then a third dataset was made by counting a reasonable number of palynomorphs, sometimes reaching more than 250



Text-fig. 2. Lithological column of the Shushan-1X well, showing the position of the studied samples, northern Western Desert, Egypt.

grains per sample, depending on the palynomorph richness status. This set was prepared only for the 40 palynomorph-productive samples. Palynomorphs were compiled in a list of genera and species (Table 1). Palynomorph data obtained throughout our study were expressed as counts and as relative percentages on distribution and semi-quantitative range charts, respectively. Data on the TPOM were presented in the ternary diagram models of Federova (1977), Duringer and Doubinger (1985) and Tyson (1993). Additional graphic presentations of palynomorphs and palynofacies were also created. The ra-

tio of marine to continental palynomorphs (m/c) was calculated by dividing the counted number of marine palynomorphs per sample by the total count of palynomorphs, multiplied by 100. Similarly, other closed-sum calculations were made for the brown wood/opaques and the phytoclasts/AOM ratios. However, all the raw data of palynomorph and palynofacies counts in this work were provided as supplements (Appendices 2 to 4). Identification of palynomorphs and other organic matter was carried out using transmitted light microscopy (Leica Microscope DM500, equipped with an ICC50 HD digital camera).

RESULTS

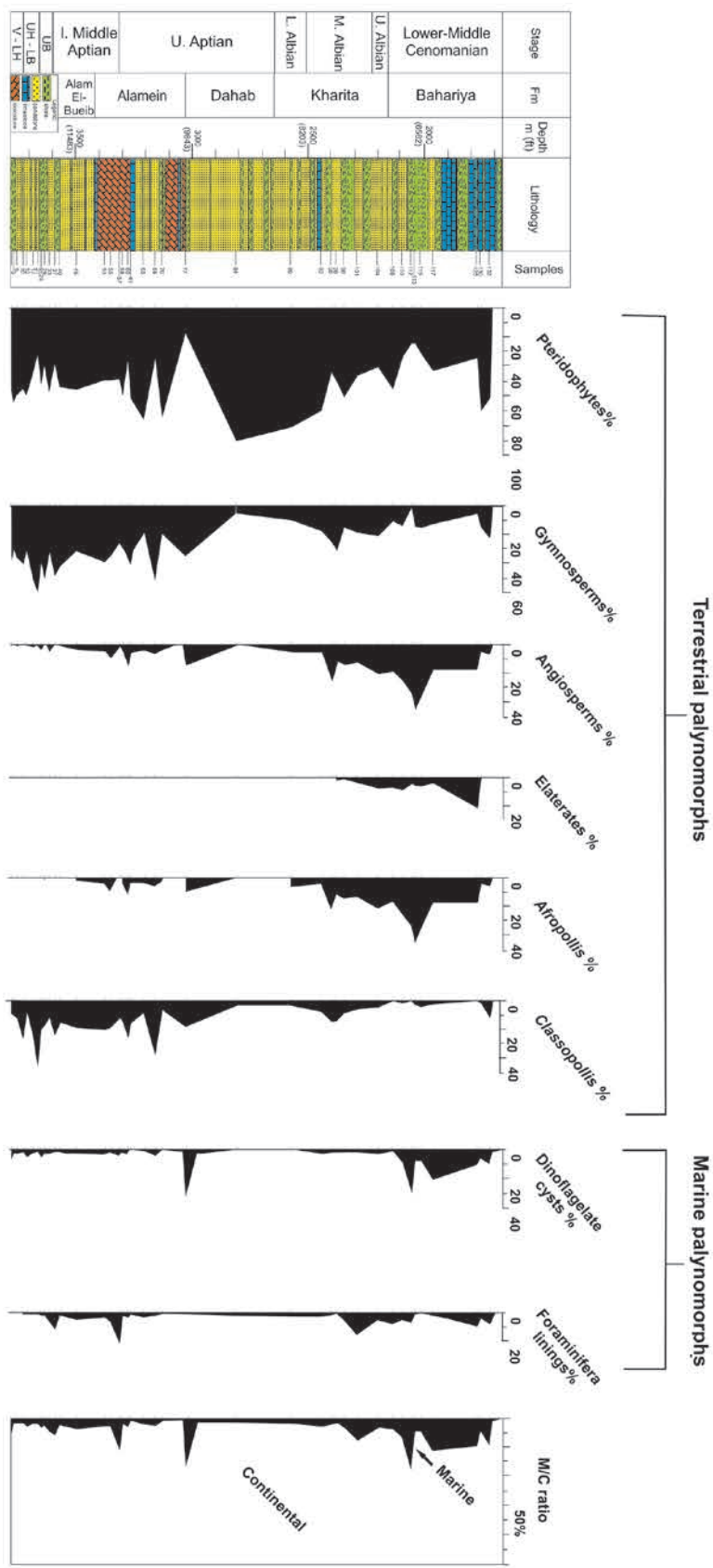
Main characteristics of the Shushan POM

Palynomorphs

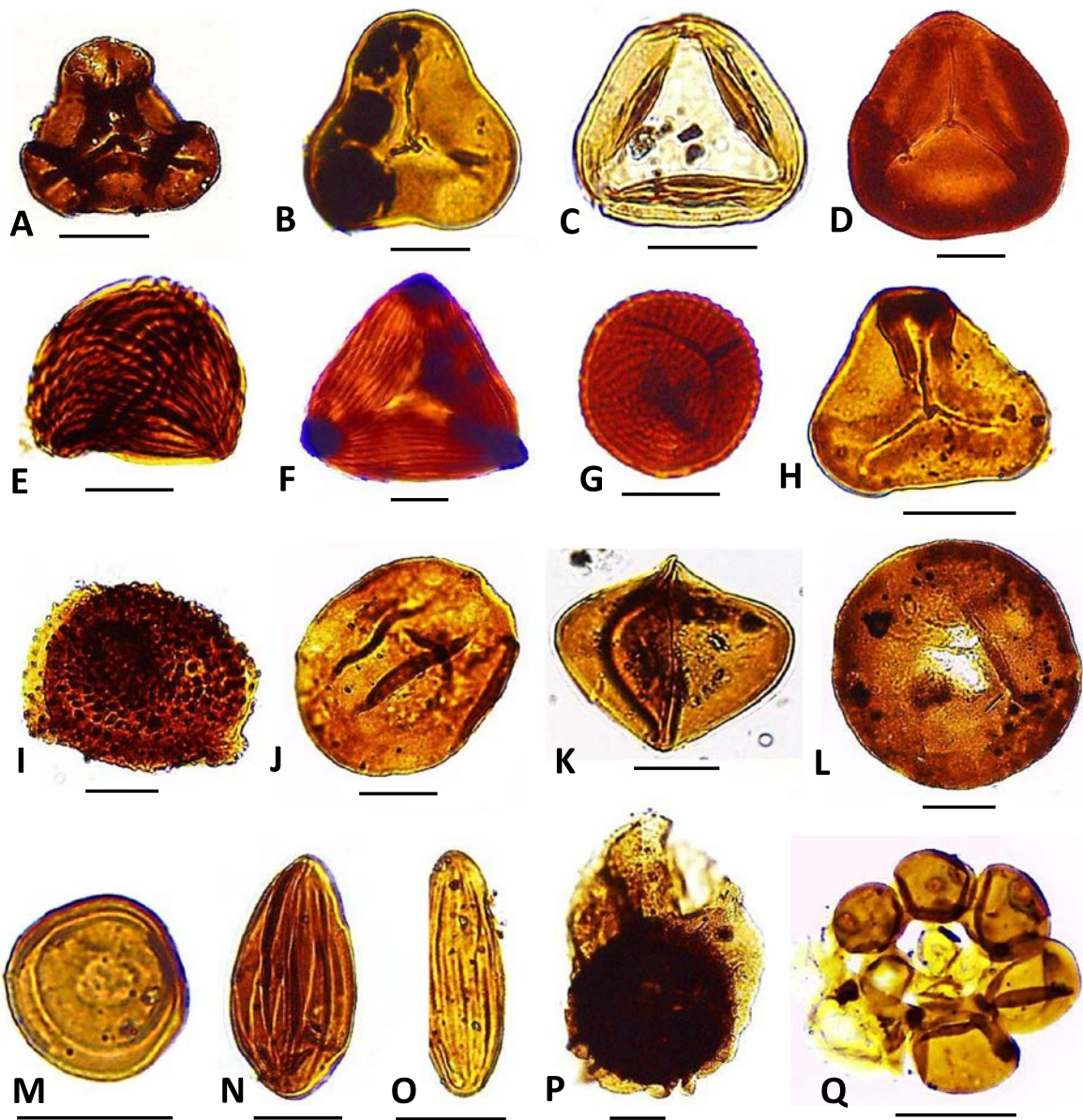
The material from the Shushan-1X well is dominated by terrestrial pollen and spores, with minor proportions of marine dinoflagellate cysts and microforaminiferal linings (Appendix 1 and Text-figs 3–6). Detailed biostratigraphy has been recently conducted by Mahmoud *et al.* (2023). The most common and abundant species throughout the whole studied interval are representatives of the fern spores *Deltoidospora*, *Triplanosporites* and *Concavissimisporites*, which constitute up to 92.2% of the total spores and pollen content. Less common are ornamented spores, i.e., *Cicatricosisporites*. Gymnosperm and angiosperm pollen show abundant and diverse distribution. One of the most important pollen grains of potential biostratigraphic significance among the gymnosperms is *Dicheiropolis etruscus*, which, although rare, occurs in the Upper Hauterivian–Lower Barremian interval of the well. The Alam El-Bueib Formation contains the highest abundances of the other gymnosperm pollen, i.e., *Classopollis* (up to 49.6% of total palynomorphs). *Araucariacites australis* is another common gymnosperm, which shows abundances up to 12.2% of total palynomorphs. Elaterite pollen grains, i.e., *Elaterosporites klaszii*, *Elaterocolpites castelainii* and *Elateroplicites africaensis* first appear in the Middle Albian (middle Kharita Formation), Upper Albian (upper Kharita Formation) and Lower–Middle Cenomanian (basal Bahariya Formation), respectively. Their abundance increases and reaches a peak in the upper Bahariya Formation (sample no. 125, 20.9% of total palynomorphs). *Ephedripites*, another gymnosperm, exhibits a percentage frequency

Spores and pollen	
1- <i>Triplanosporites</i> sp. (Text-fig. 5K)	50- <i>Retimonocolpites variiplicatus</i> Schrank and Mahmoud, 1998 (Text-fig. 6I)
2- <i>Deltoidospora</i> sp. (Text-fig. 5C)	51- <i>Tricolpites</i> spp.
3- <i>Dictyophyllidites</i> spp.	52- <i>Afropollis kahramanensis</i> Ibrahim and Schrank 1995 (Text-fig. 6E)
4- <i>Cicatricosisporites</i> sp. (Text-fig. 5E)	53- <i>Afropollis</i> sp. (Text-fig. 6B and D)
5- <i>Dictyophyllidites harrisii</i> Couper, 1958	54- <i>Foveotricolpites gigantoreticulatus</i> (Jardiné and Magloire) Schrank, 1987a–b
6- <i>Crybelosporites pannuceus</i> (Brenner) Srivastava, 1977	55- <i>Tucanopollis annulatus</i> Schrank and Mahmoud, 2002
7- <i>Deltoidospora toralis</i> (Leschik) Lund, 1977	56- <i>Stellatopollis dejaxi</i> Ibrahim, 2002a
8- <i>Todisporites minor</i> Couper, 1958	57-cf. <i>Afropollis</i> sp.
9- <i>Deltoidospora australis</i> (Couper) Pocock, 1970	58- <i>Afropollis aff. jardinius</i> Doyle <i>et al.</i> , 1982
10- <i>Concavissimisporites</i> sp.	59- <i>Retimonocolpites ghazalii</i> Ibrahim, 2002a
11- <i>Verrucosisporites</i> spp.	60- <i>Retimonocolpites pennyi</i> Schrank and Mahmoud, 2002
12- <i>Cibotiumspora jurienensis</i> (Balme) Filatoff, 1975 (Text-fig. 5A)	61- <i>Eucommiidites</i> spp.
13- <i>Auritulinaspores scanicus</i> Nilsson, 1958	62- <i>Retimonocolpites</i> sp.
14- <i>Matonisporites</i> sp.	63- <i>Dichastopollenites ghazalatensis</i> Ibrahim, 1996
15- <i>Murospora florida</i> (Balme) Pocock, 1961	64- <i>Afropollis operculatus</i> Doyle <i>et al.</i> , 1982
16- <i>Cicatricosisporites sinuosus</i> Hunt, 1985	65- <i>Stellatopollis</i> spp.
17- <i>Concavissimisporites punctatus</i> (Delcourt and Sprumont) Brenner, 1963	66- <i>Afropollis zonatus</i> Doyle <i>et al.</i> , 1982
18- <i>Deltoidospora hallii</i> Miner, 1935 (Text-fig. 5B)	67- <i>Monocolpopollenites</i> sp.
19- <i>Gleicheniidites</i> sp.	
20- <i>Kyrtomisporis</i> sp.	Dinoflagellate cysts
21- <i>Balmeisporites holodictyus</i> Cookson and Dettmann, 1958	68- <i>Subtilisphaera senegalensis</i> Jain and Millepied, 1973
22- <i>Aequitriradites norriessii</i> Backhouse, 1988	69- <i>Subtilisphaera scabrata</i> Jain and Millepied, 1973
23- <i>Biretisporites potoniaei</i> Delcourt and Sprumont, 1955	70- <i>Coronifera oceanica</i> Cookson and Eisenack, 1958 (Text-fig. 7G)
24-Echinat spores	71- <i>Subtilisphaera</i> sp.
25- <i>Concavissimisporites variverrucatus</i> Singh, 1964	72- <i>Florentinia mantellii</i> (Davey and Williams) Davey and Verdier, 1973 (Text-fig. 7F)
26- <i>Impardecispora apiverrucata</i> (Couper) Venkatachala <i>et al.</i> , 1969	73- <i>Escharisphaeridia</i> sp.
27- <i>Cicatricosisporites cf. dorogensis</i> Potonié and Gelletich, 1933	74- <i>Spiniferites</i> sp. (Text-fig. 7K)
28- <i>Aequitriradites spinulosus</i> (Cookson and Dettmann) Cookson and Dettmann, 1961	75- <i>Subtilisphaera terrula</i> (Davey) Lenten and Williams, 1976 (Text-fig. 7B)
29- <i>Pilosispores trichopapillosum</i> (Thiergart) Delcourt and Sprumont, 1955	76- <i>Coronifera albertii</i> Millioud, 1969
30- <i>Araucariacites australis</i> Cookson, 1947 ex Couper, 1953	77- <i>Oligosphaeridium complex</i> (White) Davey and Williams, 1966 (Text-fig. 7I and L)
31- <i>Classopollis classoides</i> Pflug, 1953	78- <i>Aptedinium</i> sp.
32- <i>Ephedripites</i> sp.	79- <i>Oligosphaeridium albertaine</i> (Pocock) Davey and Williams, 1969
33- <i>Cycadopites</i> sp.	80- <i>Florentinia berrani</i> Below, 1982 (Text-fig. 7M)
34- <i>Inaperturopollenites</i> Thomson and Pflug, 1953	81- <i>Subtilisphaera perlucida</i> (Alberti) Jain and Millepied, 1973 (Text-fig. 7A)
35- <i>Callialasporites</i> sp.	82- <i>Aptea polymorpha</i> Eisenack, 1958,
36- <i>Exesipollenites</i> sp.	83- <i>Oligosphaeridium diluculum</i> Davey, 1982
37- <i>Callialasporites dampieri</i> (Balme) Sukh Dev, 1961	84- <i>Pseudoceratium retusum</i> Brideaux, 1977
38- <i>Classopollis brasiliensis</i> Herngreen, 1975	85- <i>Palaeoperidinium cretaceum</i> (Pocock) Lenten and Williams, 1976
39- <i>Taxodiaceapollenites</i> sp.	86-cf. <i>Circulodinium distinctum</i> (Deflandre and Cookson) Jansonius, 1986
40- <i>Callialasporites trilobatus</i> (Balme) Sukh Dev, 1961	87- <i>Pseudoceratium securigerum</i> (Davey and Verdier) Bint, 1986
41- <i>Balmeiopsis limbatus</i> (Balme) Archangelsky, 1979 (Text-fig. 5L)	88- <i>Florentinia cooksoniae</i> (Singh) Duxbury, 1980 (Text-fig. 7N)
42- <i>Classopollis</i> sp.	89- <i>Pseudoceratium anaphrissum</i> (Sarjeant) Bint, 1986
43- <i>Taxacites sahariensis</i> Reyre, 1973	90- <i>Odontochitina operculata</i> (Wetzel) Deflandre and Cookson, 1955
44- <i>Dicheiropollis etruscus</i> Trevisan, 1972	91- <i>Cyclonephelium vannophorum</i> Davey, 1969
45- <i>Spheripollenites</i> sp.	92- <i>Cribroperidinium</i> sp.
46- <i>Elaterosporites klaszii</i> (Jardine and Magloire) Jardine 1967 (Text-fig. 6J, L, N and O)	93- <i>Cribroperidinium edwardsii</i> (Cookson and Eisenack) Davey, 1969
47- <i>Elaterocolpites castelainii</i> Jardine and Magloire, 1965 (Text-fig. 6K)	94- <i>Oligosphaeridium poculum</i> Jain, 1977
48- <i>Elateroplicites africaensis</i> Herngreen, 1973	95- <i>Circulodinium distinctum</i> (Deflandre and Cookson) Jansonius, 1986 (Text-fig. 7E)
49- <i>Afropollis jardinius</i> Doyle <i>et al.</i> , 1982 (Text-fig. 6A, C, F and G)	96- <i>Pareodinia ceratophora</i> Deflandre, 1947
	97- <i>Muderongia</i> sp.
	98- <i>Cribroperidinium orthoceras</i> (Eisenack) Davey, 1969

Table 1. List of spores, pollen and dinoflagellate cysts taxa identified in the Shushan-1X well.



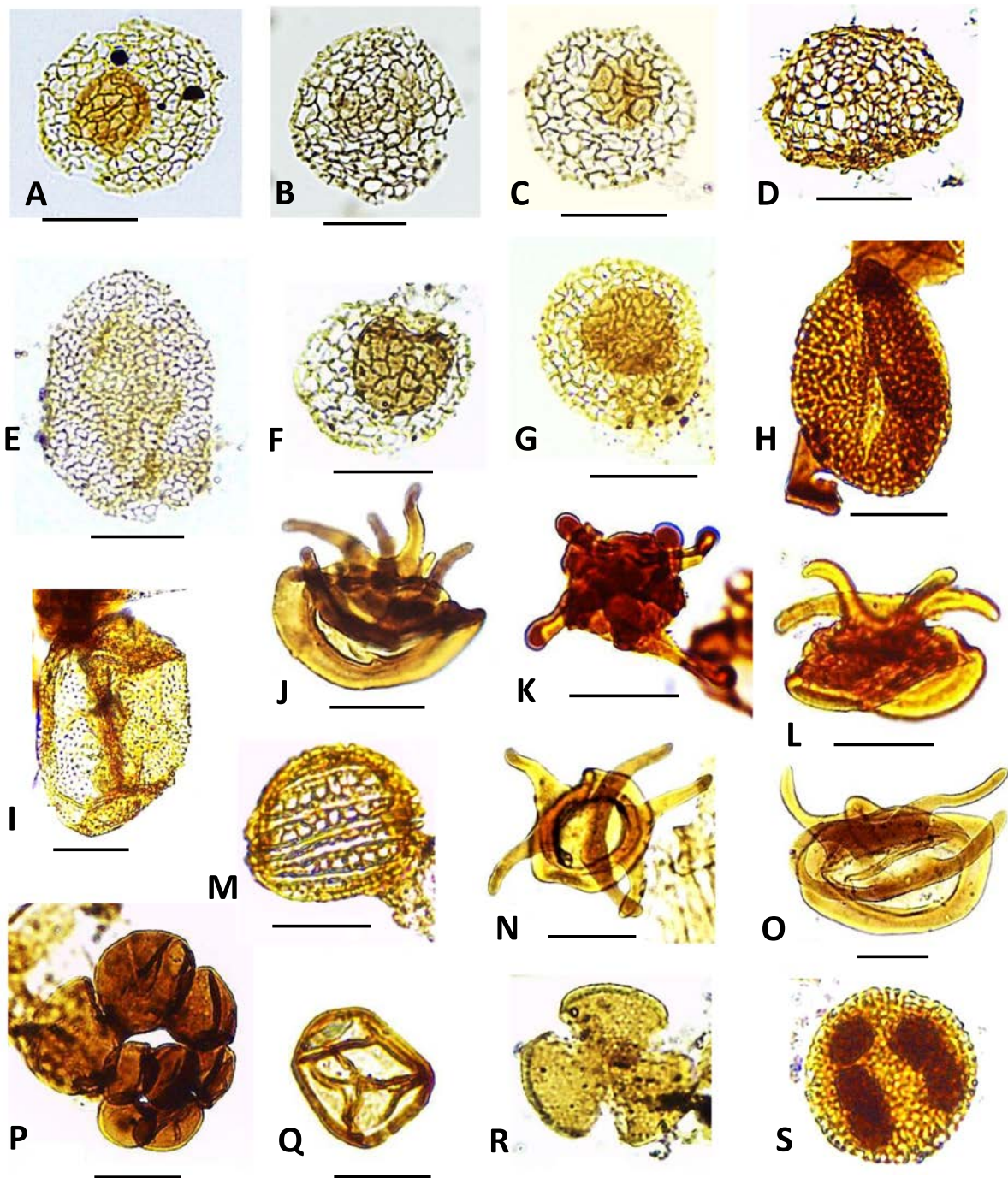
Text-fig. 3. Percentage frequencies of selected palynomorphs and palynomorph groups, with marine to continental ratios in the Shushan-1X well (for 40 samples that were counted for their palynomorph content); based on data presented in Appendices 1 and 2.



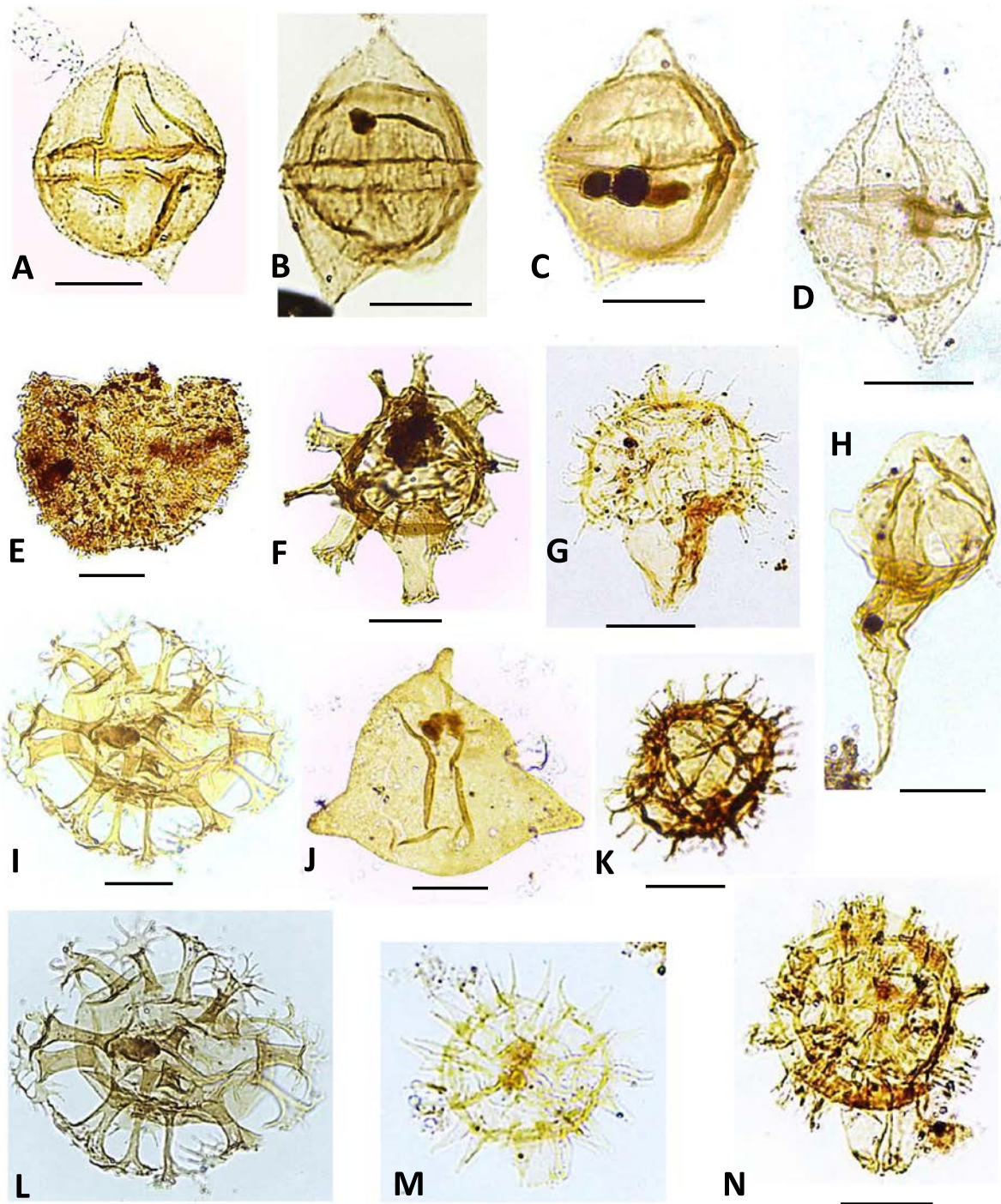
Text-fig. 4. Spores and pollen grains from the Shushan-IX well, presented with their depth, slide and sample numbers, and indices. A – *Cibotiumspora jurienensis* (Balme) Filatoff, 1975; 2,505 m, Sh-1X 1, 92, 10/150. B – *Deltoidospora hallii* Miner, 1935; 3,709 m, Sh-1X 1, 12, 10/144.5. C – *Deltoidospora* sp.; 1,679 m, Sh-1X 1, 84, 7.9/135.5. D – cf. *Kyrtomisporis* sp.; 3,630 m, Sh-1X 1, 29, 7.1/129. E – *Cicatricosisporites* sp.; 1,679 m, Sh-1X 1, 132, 18.5/151. F – *Cicatricosisporites sprumontii* Döring, 1965; 3,755 m, Sh-1X 1, 4, 13.5/146.7. G – *Cicatricosisporites orbiculatus* (Balme) Such Dev, 1961; 1,710 m, Sh-1X 2, 130, 20/143. H – *Deltoidospora toralis* (Leschik) Lund, 1977; 3,630 m, Sh-1X 1, 29, 7.1/129. I – *Aequitriradites verrucosus* (Cookson and Dettmann) Cookson and Dettmann, 1961; 3,749 m, Sh-1X 1, 5, 7/132.7. J – *Araucariacites australis* Cookson and Couper, 1953; 3,036 m, Sh-1X 2, 77, 11/150. K – *Triplanosporites* sp.; 2,813 m, Sh-1X 1, 29, 18/138. L – *Balmeiospis limbatus* (Balme) Archangelsky, 1979; 3,036 m, Sh-1X 1, 77, 12/146. M – *Classopollis* sp.; 2,405 m, Sh-1X 2, 96, 21/145. N, O – *Ephedripites* spp.; N – 1,679 m, Sh-1X 1, 132, 5.5/144.5; O – 1,710 m, Sh-1X 1, 130, 15.5/147.3. P – *Balmeiosporites holodictyus* Cookson and Dettmann, 1958; 3,761 m, Sh-1X 1, 3, 13/150. Q – Planispiral microforaminiferal lining; 2,085 m, Sh-1X 1, 112, 13/134.5. Scale bars = 20 µm.

mostly below 15% of total sporomorphs and reaches a maximum abundance in the Upper Barremian (upper Alam El-Bueib Formation). Several species of the angiosperm pollen *Afropollis* show a common

to abundant distribution, starting from the Aptian (Alamein Formation) onwards until the end of the studied borehole interval. Their abundances increase and reach a primary peak, made up of *Afropollis jar-*



Text-fig. 5. Pollen grains from the Shushan-1X well, presented with their depth, slide and sample numbers, and indices. A, C, F, G – *Afropollis jardinius* Doyle, Jardin and Doerenkamp, 1982; A – 2,070 m, Sh-1X 1, 113, 14/145; C – 2,307 m, Sh-1X 1, 101, 8/150.4; F – 2,222 m, Sh-1X 1, 104, 18/152; G – 2,222 m, Sh-1X 1, 104, 19.2/139. B, D – *Afropollis* sp.; B – 2,033 m, Sh-1X 1, 115, 19/143; D – 2,033 m, Sh-1X 1, 115, 11/133.1. E – *Afropollis kahramanensis* Ibrahim and Schrank, 1995; 2,033 m, Sh-1X 1, 115, 20/145. H – *Retimonocolpites* sp. 1 of Schrank and Mahmoud (2002); 1,710 m, Sh-1X 1, 110, 9/138. I – *Retimonocolpites variplicatus* Schrank and Mahmoud, 1998; 2,417 m, Sh-1X 1, 95, 20/149.5. J, L, N, O – *Elaterosporites klaszii* (Jardiné and Magloire) Jardiné, 1967; J – 2,222 m, Sh-1X 1, 104, 11/151; L – 2,115 m, Sh-1X 2, 110, 14/136; N – 2,070 m, Sh-1X 1, 113, 15.4/138; O – 2,070 m, Sh-1X 1, 113, 16/135. K – *Elaterocolpites castelainii* Jardiné and Magloire, 1965; 2,115 m, Sh-1X 1, 110, 11.2/141. M – indeterminate pollen grain (?*Trisectoris* sp.); 2,813 m, Sh-1X 1, 84, 11.5/144. P – Planispiral microforaminiferal linings; 3,036 m, Sh-1X 1, 77, 19.1/140. Q – indeterminate pollen grain (cf. *Araucariacites* sp.); 3,709 m, Sh-1X 2, 12, 12.8/145. R – *Tricolpites sagax* Norris, 1967; 2,149 m, Sh-1X 2, 108, 16/136. S – cf. *Retiacolpites columellatus* Schrank in Schrank and Mahmoud, 2002; 2,222 m, Sh-1X 1, 104, 2.5/141.1. Scale bars = 20 µm.



Text-fig. 6. Dinoflagellate cysts from the Shushan-1X well, presented with their depth, slide and sample numbers, and indices. A – *Subtilisphaera perlucida* (Alberti) Jain and Millepied, 1973; 3,036 m, Sh-1X 1, 77, 20.5/139. B – *Subtilisphaera terrula* (Davey) Lentin and Williams, 1976; 3,036 m, Sh-1X 1, 77, 11.5/132.5. C – *Subtilisphaera cf. terrula* (Davey) Lentin and Williams, 1976; 3,036 m, Sh-1X 2, 77, 8/145. D – *Subtilisphaera cheit* Below, 1981; 3,036 m, Sh-1X 2, 77, 15/139.6. E – *Circulodinium distinctum* (Deflandre and Cookson) Jansonius, 1986; 3,709 m, Sh-1X 3, 12, 21/142. F – *Florentinia mantelli* (Davey and Williams) Davey and Verdier, 1973; 3,036 m, Sh-1X 2, 77, 8.5/132.5. G – *Coronifera oceanica* Cookson and Eisenack, 1958; 1,710 m, Sh-1X 1, 130, 12.1/144. H – side view of *Odontochitina operculata* (Wetzel) Deflandre and Cookson, 1955; 3,661 m, Sh-1X 1, 21, 10.9/135. I, L – *Oligosphaeridium complex* (White) Davey and Williams, 1966; I – 3,502 m, Sh-1X 2, 45, 13.2/148; L – 3,036 m, Sh-1X 2, 77, 10/142. J – *Pseudoceratium cf. securigerum* (Davey and Verdier) Bint, 1986; 3,362 m, Sh-1X 1, 55, 23/144. K – *Spiniferites* sp., specimen with short processes; 3,036 m, Sh-1X 2, 77, 19/145. M – *Florentinia berran* Below, 1982; 3,036 m, Sh-1X 2, 110, 6/147.5. N – *Florentinia cooksoniae* (Singh) Duxbury, 1980; 3,036 m, Sh-1X 2, 77, 11.5/133. Scale bars = 20 µm.

dinus/A. kahramanensis (44.5 of total palynomorphs; Lower–Middle Cenomanian, Bahariya Formation, sample no. 113).

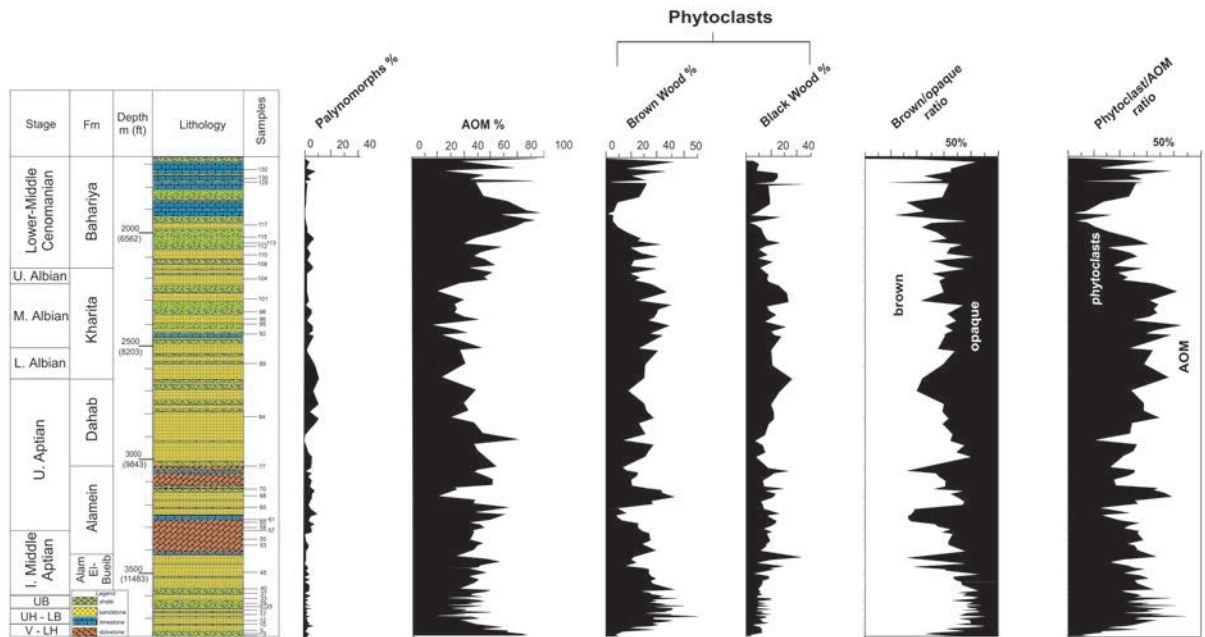
Two horizons in the Dahab (sample no. 77; depth 3,036 m) and Bahariya (samples no. 112; depth 2,085) formations show a dramatic increase in the abundance of dinoflagellate cysts (32% and 29.6% of total palynomorphs, respectively). In spite of this abundant occurrence, the diversity pattern in these two horizons varies considerably from high (Dahab Formation) to poor (Bahariya Formation). Both gonyaulacoid (e.g., *Oligosphaeridium*, *Florentinia*) and peridinoid (*Subtilisphaera*) cysts occur, with few ceriatoids (*Muderongia*). Microforaminiferal linings reach percentages up to 19.8% (sample no. 57; depth 3,319 m) and 15.7% (sample no. 101; depth 2,307 m) of total palynomorphs in the Alamein and Kharita formations, respectively. At these two levels, dinoflagellate cysts are obviously rare (3.6% and 1.6% of total palynomorphs, respectively) and are very poorly diversified.

Palynofacies

Palynomorphs show extremely rare percentage frequencies because they are masked by AOM and phytoclasts (Text-fig. 7). In this context, brown/black wood and AOM dominate the palynofacies and display a monotonous abundance pattern of interchanging fluctuating proportions. At some stratigraphic levels one of these two components dominates the other.

Some minor fractions of the total count of TPOM surpass 0.1%, such as cuticles at depths 2,368 m and 3,591 m. This minority of cuticles might be attributed to the degradation of their original component. Scolecodonts (depths 3,036 m and 2,085 m), fungal spores (depths 1,817 m and 2,813 m), *Chomotriletes minor* (depths 1,710 m and 3,578 m), *Ovoidites parvus* (depth 1,679 m), *Veryhachium valiente* (depth 2,033 m) and *Botryococcus* spp. (depth 3,307 m) are minor components of the recorded TPOM. These secondary palynofacies categories collectively attain percentage frequencies that are graphically not representable (below 1% of total palynofacies).

At the base of the Alam El-Bueib Formation, the palynofacies is relatively dominated by AOM. In the overlying Alamein Formation, phytoclasts and AOM display observable interchanging fluctuations; lath-shaped and equidimensional phytoclasts occur. However, in the overlying Dahab Formation, AOM is the predominant palynofacies element. Phytoclasts prevail in the Kharita Formation, whereas in its top AOM gradually increases to a domination of the association. AOM reaches a maximum in the middle part of the overlying Bahariya Formation. Phytoclasts increase again in the topmost part of the section in this rock unit. The brown-to-opaque wood ratio generally declines with increasing AOM throughout the whole succession, especially in the Bahariya Formation. AOM shows inclusions of pyrite crystals at some levels.



Text-fig. 7. Percentage abundances of palynomorphs, particulate organic matter, brown/opaque ratio, and phytoclasts/AOM ratio of the Shushan-1X well, northern Western Desert, Egypt.

DISCUSSION

Paleoenvironmental interpretation

Our main approach to the interpretation of the depositional environment relies essentially on the compositional development of the TPOM. Palynofacies and palynomorphs may thus provide significant information on the depositional environments (e.g., Lister and Batten 1988; Tyson 1995; Mahmoud *et al.* 2017, 2019). Generally, TPOM was derived essentially from land vegetation (e.g., wood phytoclasts, spores and pollen) and marine sources (e.g., microforaminiferal test linings and dinoflagellate cysts).

In normal (open) marine environments, the marine components are common constituents of the palynofacies. In near-shore (proximal) and/or marginal marine settings, which is the case here, the marine components significantly decline. The high terrigenous influx of sedimentary organic matter (SOM) in the proximal sites dilutes the concentration of palynomorphs and obscures their distribution. Roncaglia and Kuijpers (2006) stated that the palynological model of Tyson (1993) showed good potential for characterizing marine, high-latitude facies deposited distally on the shelf, but is inadequate for facies deposited proximally. Therefore, we used the model of Tyson only to understand the redox states. On the other hand, Roncaglia and Kuijpers's (2006) model cannot be applied in this study due to the variability between SOM nature and distribution in high latitudes and in the present (Tethyan) area. In part, we have used the latter model to discriminate between proximal and distal settings.

Palynomorphs inferences

In general, the low diversity of dinoflagellate cyst assemblages across the investigated section suggests restricted marine environments, as seen in the regional record (e.g., Uwins and Batten 1988; Omran *et al.* 1990; Schrank and Mahmoud 1998; Mahmoud *et al.* 2019). The poor state of preservation and the reduced length of processes are prominent features of the Shushan dinoflagellate associations. Reduced process lengths in dinoflagellates can be attributed to restricted marine environments of reduced salinities. Some skolochorate *Florentinia* cysts have relatively short processes, with lengths less than half cyst diameter. It is believed that these cysts responded to such restricted environments of lower than normal marine salinities. Process length variation has been observed for *Lingulodinium machaerophorum* in

Holocene surface sediments and was potentially used as a salinity indicator (Mertens *et al.* 2009). However, the relative high abundances of dinoflagellate cysts in the Dahab (only one horizon) and Bahariya formations, suggest periods of open marine conditions.

The absence of chorate cysts such as *Florentinia* and *Coronifera* cysts indicate a stressed marginal marine environment of below-normal marine salinity in the Alam El-Bueib and Alamein formations (Batten 1983; Lister and Batten 1988). The scarcity and fragmentary occurrences of *Oligosphaeridium* spp. in these two rock units is consistent with their restricted nature. They range between 0.4% of total palynomorphs (sample no. 58, depth 3,307 m) to a maximum single value of 1.6% of total palynomorphs (sample no. 57, depth 3,319 m). *Oligosphaeridium* and *Florentinia* are cysts indicative of open marine conditions (e.g., Omran *et al.* 1990; Carvalho *et al.* 2016, see discussion below). However, the idea that this marginal setting has a brackish nature is based on the presence of the dinoflagellate cysts *Subtilisphaera* and *Muderongia* (e.g., Piasecki 1984; Harding 1986; Mahmoud *et al.* 2017). Increase in the abundance of microforaminiferal linings in a few horizons of the Alamein Formation cannot indicate a specific setting since they come from a wide range of habitats (Lejzerowicz *et al.* 2010). At depth 3,319 m (sample no. 57) these foraminifers dominate (c. 23.4% of total palynomorphs) over dinoflagellate cysts (c. 3.6% of total palynomorphs).

As indicated earlier above, the Alamein Formation was inferred to have accumulated in shallow marine to deltaic environments, over wide areas of the northern Western Desert of Egypt (e.g., Kerdany and Cherif 1990). The global Late Barremian–Aptian marine transgression (see Vail *et al.* 1977; Van der Meer *et al.* 2022) is believed to have influenced the area of northern Egypt later by the advent of the Aptian. It has resulted in the deposition of the ‘upper’ carbonate interval of the Alamein Formation under marine settings. The obtained data confirm the previous concept of Mahmoud *et al.* (2017) that local tectonics were not responsible for the marine transgression in the area.

In a single horizon in the Dahab Formation, an abundant and diverse assemblage of gonyaulacoid dinoflagellate cysts with *Oligosphaeridium*, *Florentinia* and *Coronifera* (32% of total palynomorphs, sample no. 77, depth 3,036 m) is associated with a low terrestrial palynomorph content. Where open-marine conditions are inferred, these cysts are common. The *Oligosphaeridium* community in this interval contains *O. albertense*, *O. complex* and *O.*

diloculum, with long processes, a feature assumed to be indicative of open-marine (neritic) conditions (e.g., Carvalho *et al.* 2016). This again reflects the impact of a global (Late Barremian–Aptian) eustatic sea level rise, which brought a normal marine environment (e.g., Mutterlose and Harding 1987; Habib *et al.* 1992) in this stratigraphic horizon.

The Kharita Formation witnessed a sharp upward decline in the abundance and diversity of dinoflagellate cysts (4 species), suggesting very shallow to coastal marine conditions. This may also be related to the global and Egyptian drop in sea level by the end of the Aptian (see Said 1990). However, the magnitude of transgressive/regressive impacts does not reflect good correlation. This can be seen from the occurrence of these shallower settings, which were already in existence during the deposition of the underlying Dahab Formation. It is suggested therefore that the local paleotopography of the northern Western Desert area, where the investigated bore-hole was drilled, played the major role. In support, *Elaterosporites* and *Afropollis* pollen grains are indicative of such nearshore (coastal) conditions (see Schrank 2001).

Despite being low-diversity, the abundant dinoflagellate associations (up to 29.6% of total palynomorphs, sample no. 112, depth 2,058 m) in the Bahariya Formation indicate vertical development of the distal inner shelf environment (e.g., Tyson 1995; Batten 1999). These associations are dominated by *Subtilisphaera* and spiniferate cysts. As discussed above, *Subtilisphaera* is indicative of marginal settings, but its association with spiniferate cysts suggests a marine environment, somewhat differing from that seen in the underlying Dahab Formation. The occurrence of *Spiniferites*, along with some relatively long-process cyst types such as *Florentinia* and *Coronifera*, can be considered typical of the open marine environment (e.g., Dale 1983; Omran *et al.* 1990; Carvalho *et al.* 2016). *Spiniferites* species prefer normal salinity and oxygenation in neritic to nearshore shallow-water environments (Prauss 2001). In modern sediments, species of *Spiniferites* were observed in coastal environments of full marine conditions and in open oceans as well (Zonneveld *et al.* 2013). This upward transition is consistent with a change in the sedimentary facies from coarse sandstones and siltstones to fine shales and carbonates as a response to increasing depth of the depositional sites (e.g., Vallejo *et al.* 2002; Carvalho *et al.* 2006). This is believed also to be associated with the global Late Cenomanian marine transgression, which covered most of northern Egypt during that time (Vail

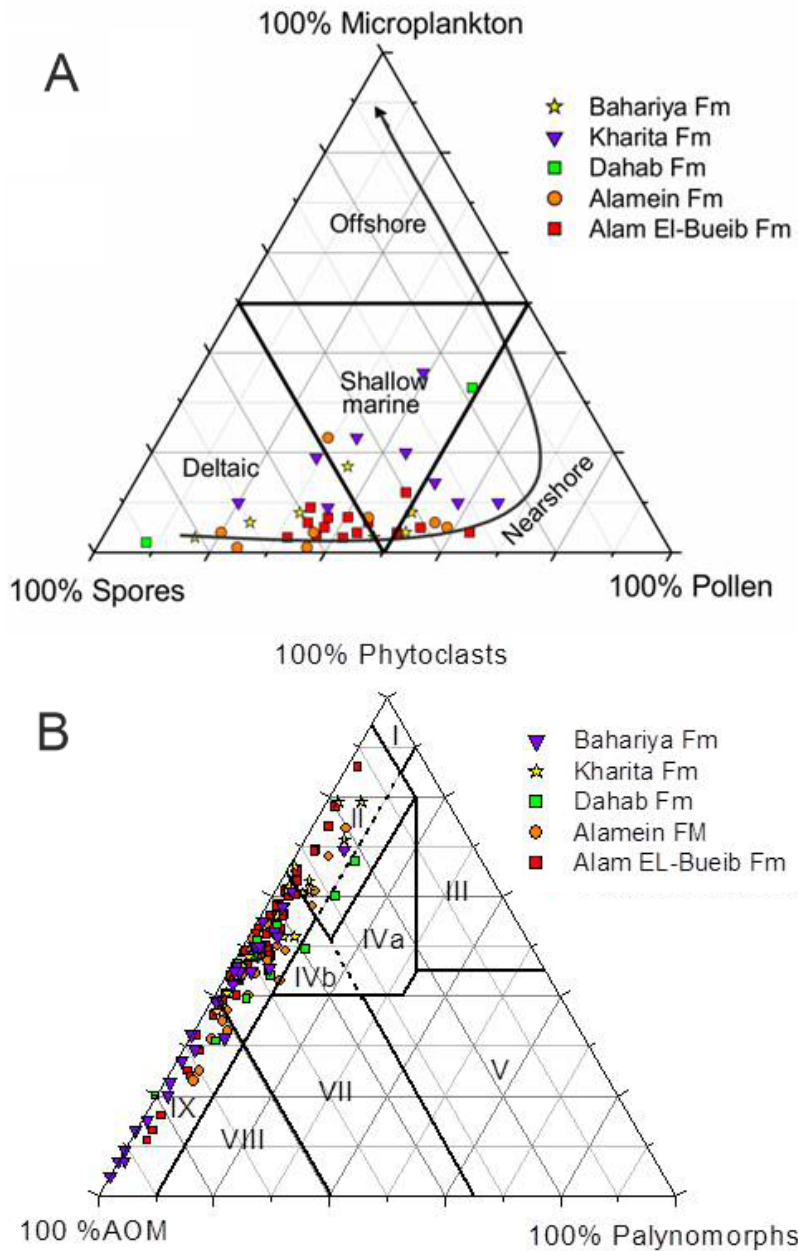
et al. 1977; Guiraud and Bosworth 1999; Guiraud *et al.* 2001).

Miospores reflect humid conditions, as can be indicated by the rich fern spores throughout the whole investigated well section (up to 92.2% of total spores and pollen). Similar qualitative and quantitative results were previously documented from these northern basins (e.g., El-Soughier *et al.* 2010, Matruh Basin; Mahmoud *et al.*, 2019, 2023, Shushan Basin; El Atfy 2021, Faghur Basin). Abundant *Classopollis* (*Cheirolepidiaceae*) pollen is associated with these ferns, especially in the Alam El-Bueib, Alamein and Dahab formations (up to 51.4% of total spores and pollen; 49.6% of total palynomorphs). *Classopollis* was frequently reported from Lower Cretaceous rocks in Egypt (e.g., Schrank and Mahmoud 1998; Mahmoud *et al.* 2023). Lower percentages of this pollen occur in the slightly wetter (hot) tropical regions of Africa (Doyle 1999). The abundance of *Ephedripites* and *Classopollis* pollen was interpreted by Schrank and Nesterova (1993) as indicative of xerophytic and drier conditions. However, *Classopollis* pollen in our material is associated with abundant humidity-loving fern spores in most of the investigated section. Therefore, *Classopollis* may be questionably considered here as an indicator of aridity. Probably, *Classopollis* pollen adapted and flourished with increasing humidity. In support of this view, ephedroid pollen (xerophytes) declines where the associated *Classopollis* reaches its maximum abundance. Furthermore, where ephedroids are relatively rare, ferns and *Classopollis* still show appreciable percentages. Based on this and previous paleo-latitudinal records of *Classopollis*, we believe that this pollen can thrive in both arid and humid habitats.

Palynofacies inferences

Environmental gradients based on plotting the investigated samples on ternary diagrams (Text-fig. 8) for each of the recognized formations penetrated by the Shushan-1X well can be interpreted as follows:

The Alam El-Bueib Formation (Text-fig. 8A) enters fields II, VI and IX. This reflects distal suboxic-anoxic environments, sometimes partly marginal dysoxic-anoxic in a few levels. The formation reflects high AOM content (>50% of total palynofacies) and low to zero marine components. On the SMP diagram (Text-fig. 8B), samples of the formation occupy the deltaic and near-shore fields, confirming again a general proximal deposition of the formation. One sample shows a relatively high abundance of marine



Text-fig. 8. Ternary diagrams for the Shushan-1X well. A – SMP (spores, pollen, microplankton) ternary diagram (after Duringer and Doubinger 1985), based on data provided in Appendix 3. B – AOM-palynomorph/phytoclast ternary diagram of particle frequency (percentage of TPOM), with palynofacies fields of Tyson (1993), based on data provided in Appendix 4.

microplankton (foraminiferal linings and dinoflagellate cysts, 12% of total palynomorphs), which occupy the middle (shallow marine) area of the diagram. Microforaminiferal linings, in particular, are known to decrease in abundance in marginal marine conditions and increase in normal marine settings (Lister and Batten 1988; Stancliffe 1989).

The Alamein Formation samples enter the same previous fields on the APP diagram, which suggests also suboxic-anoxic states at the base of the formation. Then the redox states return to dysoxic-anoxic conditions at the top. A very high terrestrial freshwater influx has been documented in this rock unit. On the SMP diagram, samples of the formation occupy

the shallow marine to deltaic near-shore sites. An exception is at the base, where the ratio of marine microplankton increases (up to 23% of total palynomorphs), and in which open (shallow) marine conditions might have developed.

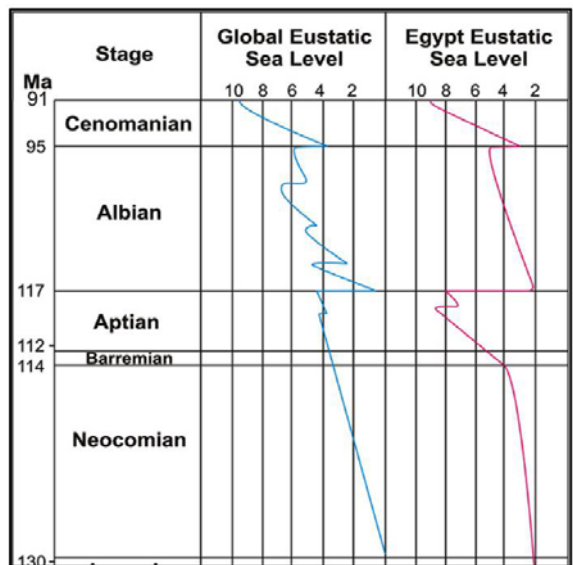
Samples of the Dahab Formation plotted on the APP diagram reflect the same conditions interpreted for the previously described Alam El-Bueib Formation, except for the lowermost interval that exhibits more proximal settings with high terrestrial influx. On the SMP diagram, the samples occupy the shallow marine to deltaic area. Sample no. 77 (depth 3,036 m) notably reflects a relatively offshore distal shelf environment due to the high abundance and diversity of the dinoflagellate cysts and foraminiferal linings (up to 33% of total palynomorphs).

On the APP and TPOM ternary plots, samples of the Kharita Formation show previous conditions, but in the form of repeated fluctuations across the whole investigated rock interval of the formation. Most of the samples reflect a very high terrestrial influx. On the SMP diagram, samples of this rock unit lie in the deltaic and near-shore fields. The topmost sample reflects a more distal setting, where the percentage of microplankton increases to as much as 17% of total palynomorphs.

The Bahariya Formation samples show the same previous characteristics and environmental preferences. However, AOM displays extraordinary amounts associated with anoxia (up to 96% of total palynofacies) and low terrestrial influx. On the SMP diagram, samples of this unit occupy the near-shore area and become deeper, more distal, at the top. The brown to black ratio drops markedly with increasing AOM in this unit, which indicates far offshore deposition (Habib 1982; Summerhayes 1987; Tyson 1989; Götz *et al.* 2005). A drop in the brown/black wood ratio in these predominantly shale/carbonate lithologies can therefore be attributed to a basinward setting and low-energy finer marine sediments (Habib 1983; Firth 1993; Tyson 1995), rather than being related to an increasing sand content.

The Shushan paleoenvironment in a basinal context

Temporal and spatial changes in the ratio of marine to continental palynomorphs can be used to identify proximal-distal sedimentation trends (Steffen and Gorin 1993; Pittet and Gorin 1997). This ratio is relatively affected by taphonomic processes (Bombardiere and Gorin 2000). Therefore, it could only be applied to the same basin with pre-



Text-fig. 9. Global and Egyptian Early Cretaceous eustatic sea level cycles (after Vail *et al.* 1977, and Said 1990, respectively).

sumably similar taphonomic properties. This ratio is relatively higher than that in the east and southeast of the Shushan Basin (2.6/97.4 to 11.9/88.1% in the Alam El-Bueib Formation, 1.2/98.8 to 23.4/76.6% in the Alamein Formation, 1.9/98.1 to 32.9/67.1% in the Dahab Formation, 2.9/97.1 to 17.3/82.7% in the Kharita Formation, and 8.8/91.3 to 36.3/63.7% in the Bahariya Formation). This is an indication of more offshore conditions in the west, which can be exemplified by the occurrence of open marine palynoflora in the Dahab Formation. The higher m/c ratios in the Dahab and Bahariya formations correlate with the global Aptian and Cenomanian marine transgressions, respectively (Text-fig. 9), which covered most of the northern Egypt area during these times (Vail *et al.* 1977; Guiraud and Bosworth 1999; Guiraud *et al.* 2001). However, the Alam El-Bueib Formation shows m/c ratios comparable to those from the east and southeast of the basin, whereas in the Shushan-IX well, the Alamein, Dahab and Kharita formations show higher marine percentages. In conclusion, the paleoenvironmental setting in the west of the basin was more distant from the land than in the east and southeast of the basin. Mahmoud *et al.* (2019) correlated the pre-Cenomanian Lower Cretaceous rock units across the east-southeast-west Shushan Basin and considered the Alam El-Bueib Formation to indicate shallow settings in the southeast. This is reflected in the lower marine ratio, the occurrence of brackish

dinoflagellate cyst types, and the dominance of terrestrial palynomorphs. The presence of an unconformity surface at the base of the overlying Alamein Formation in the investigated well section confirms this interpretation. In conclusion, by incorporating current results with previously established information (e.g., Mahmoud et al. 2019), we suggest that sedimentation in the west was continuous across the whole investigated interval in the Shushan Basin, without any detectable major hiatuses.

CONCLUSIONS

Our present palynological criteria suggest a predominant proximal depositional setting of the investigated Valanginian to Cenomanian sequence of the Shushan-1X well. Periods of inner shelf environments can be seen in some horizons in the Dahab (Aptian) and Bahariya (Lower–Middle Cenomanian) formations, frequently described from the northern basins of Egypt (e.g., Abdel-Kireem et al. 1996; El Beialy et al. 2011; El-Soughier et al. 2014; Mahmoud et al. 2017, 2019; El Atfy 2021). The high terrestrial influx in the restricted (marginal) environment masks the quantitative distribution pattern of palynofacies and, consequently, hampers the full application of Tyson's (1993) ternary model. The more open (shallow) marine environment can hardly be reflected by palynomorphs alone. We recommend integrating palynomorph and palynofacies data together for better environmental reconstruction. We believe that the redox states were not responsible for the low diversity and abundance of the dinoflagellate cysts. They may have been influenced by environmental restrictions. The nature of marginal settings is not suitable for dinoflagellates to thrive and diversify. Consequently, many Cretaceous cosmopolitan species were not encountered in our samples. A drop in the m/c ratio seems to be consistent with the poor and low diversity nature of the dinoflagellate cyst associations. Conversely, higher m/c values observed in some stratigraphic levels suggest strong relationships with both global and Egyptian Cretaceous eustatic sea-level cycles. Many of the palynofacies categories reflect rare distribution, although they are frequently recovered from sediments infilling the basin. Cuticles, for example, might have degraded to AOM, in which their original structures were completely destroyed. In this case, altered AOM, with its original source either from land-plants (e.g., cuticles) or from aquatic palynomorphs, remains enigmatic.

Acknowledgments

Thanks are due to the Egyptian General Petroleum Corporation (E.G.P.C.), for providing the material for the present study. We are deeply indebted to Anna Żylińska (Editor), Przemysław Gedl (Polish Academy of Science, Kraków, Poland) and an anonymous reviewer for critical remarks and improvement of the manuscript.

REFERENCES

- Abdel-Kireem, M., Schrank, E., Samir, A. and Ibrahim, M. 1996. Cretaceous palaeoecology, palaeogeography and palaeoclimatology of the northern Western Desert, Egypt. *Journal of African Earth Sciences*, **22**, 93–112.†
- Batten, D. 1983. Identification of amorphous sedimentary organic matter by transmitted light microscopy. *Special Publications of the Geological Society, London*, **12**, 275–287.
- Batten, D. 1999. Palynofacies analysis. In: Jones, N.P. and Rowe, N.P. (Eds), *Fossil Plants and Spores: Modern Techniques*, 194–198. Geological Society of London; London, Bath.
- Bombardiere, L. and Gorin, G. 2000. Stratigraphical and lateral distribution of sedimentary organic matter in Upper Jurassic carbonates of SE France. *Sedimentary Geology*, **132**, 177–203.†
- Carvalho, M., Filho, J. and Menezes, T. 2006. Paleoenvironmental reconstruction based on palynofacies analysis of the Aptian–Albian succession of the Sergipe Basin, Northeastern Brazil. *Marine Micropaleontology*, **59**, 56–81.
- Carvalho, M.A., Bengtson, P. and Lana, C.C. 2016. Late Aptian (Cretaceous) paleoceanography of the South Atlantic Ocean inferred from dinocyst communities of the Sergipe Basin, Brazil. *Paleoceanography*, **31**, 2–26.
- Dale, B. 1983. Dinoflagellate resting cysts: ‘benthic plankton’. In: Fryxel, G.A. (Ed.), *Survival Strategies of the Algae*, 69–136. Cambridge University Press; Cambridge.
- Doyle, J. 1999. The rise of angiosperms as seen in the African Cretaceous pollen record. In: Heine, K. (Ed), *Third Conference on African Palynology*, Johannesburg, 14–19 September, 1997, 3–29. Balkema; Rotterdam.
- Duringer, P. and Doubinger, J. 1985. La palynologie: un outil de caractérisation des faciès marins et continentaux à la limite Muschelkalk supérieur-Lettenkohle. *Sciences Géologiques, Bulletins et Mémoires*, **38**, 19–34.
- El Atfy, H. 2021. Palynofacies as a paleoenvironment and hydrocarbon source potential assessment tool: An example from the Cretaceous of north Western Desert, Egypt. *Palaeobiodiversity and Palaeoenvironments*, **101**, 35–50.
- El Atfy, H., Ghassal, B., Maher, A., Hosny, A., Mostafa, A., and Littke, R. 2019. Palynological and organic geochemical studies of the Upper Jurassic–Lower Cretaceous succes-

- sions, Western Desert, Egypt: Implications for paleoenvironment and hydrocarbon source rock potential. *International Journal of Coal Geology*, **211**, 103207.
- El Atfy, H., Ghassal, B. and Littke, R. 2023. Petroleum source rocks of Egypt: an integrated spatio-temporal palynological and organic geochemical studies within the Phanerozoic. In: Hamimi, Z., Khozeym, H., Adatte, T., Nader, F.H., Oboh-Ikuenobe, F., Zobaa, M.K. and El Atfy, H. (Eds), *The Phanerozoic Geology and Natural Resources of Egypt*, 649–674. Springer Link; Cham.
- El Beialy, S., El Atfy, H., Zavada, M., El Khoriby, E. and Abu Zied, R. 2010. Palynological, palynofacies, paleoenvironmental and organic geochemical studies on the Upper Cretaceous succession of the GPTSW-7 well, north Western Desert, Egypt. *Marine and Petroleum Geology*, **27**, 370–385.
- El Beialy, S., El-Soughier, M., Mohsen, S. and El Atfy, H. 2011. Palynostratigraphy and paleoenvironmental significance of the Cretaceous succession in the Gebel Rissu-1 well, north Western Desert, Egypt. *Journal of African Earth Sciences*, **59**, 215–226.
- El-Soughier, M., Mahmoud, M. and Li, J. 2010. Palynology and palynofacies of the Lower Cretaceous succession of the Matruh2-1X borehole, northwestern Egypt. *Revista Española de Micropaleontología*, **42**, 37–58.†
- El-Soughier, M., Deaf, A. and Mahmoud, M. 2014. Palynostratigraphy and palaeoenvironmental significance of the Cretaceous palynomorphs in the Qattara Rim-1X well, North Western Desert, Egypt. *Arabian Journal of Geosciences*, **7**, 3051–3068.
- Federova, V. 1977. The significance of the combined use of microphytoplankton, spores, and pollen for differentiation of multi-facies sediments. In: Samoilovich, S. and Timoshina, N. (Eds), *Questions of Phytostratigraphy*. Trudy Neftyanogo Nauchno-Issledovatel'skogo Geologorazvedochnogo Instituta (VNIGRI), **398**, 70–88.
- Firth, J. 1993. Palynofacies and thermal maturation analysis of sediments from the Nankai Trough. In: *Proceedings of the Ocean Drilling Program, Scientific Results*, **131**, 57–69.
- Ghorab, M., Ebeid, Z. and Tawfik, N. 1971. On the stratigraphy of the northeastern corner of the Western Desert. 9th Annual Meeting of Geological Society of Egypt, Giza. Egypt, Survey Department, Egypt, 48 p.
- Götz, A., Szulc, J. and Feist-Burkhardt, S. 2005. Distribution of sedimentary organic matter in Anisian carbonate series of S Poland: Evidence of third order sea-level fluctuations. *International Journal of Earth Sciences (Geologische Rundschau)*, **94**, 267–274.
- Guiraud, R. and Bosworth, W. 1999. Phanerozoic geodynamic evolution of northeastern Africa and the northwestern Arabian platform. *Tectonophysics*, **315**, 73–104.†
- Guiraud, R., Issawi, B., Bosworth, W., Ziegler, P., Cavazza, W., Robertson, A., and Crasquin-Soleau, S. 2001. Phanerozoic history of Egypt and surrounding areas. *Peri-Tethys Memoir*, **6**, 469–509.†
- Habib, D. 1982. Sedimentary supply origin of Cretaceous black shales. In: Schlanger, S.O. and Cita, M.B. (Eds), *Nature and origin of Cretaceous carbon-rich facies*, 113–127. Academic Press; New York.
- Habib, D., 1982. Sedimentary supply origin of Cretaceous black shales. In: Schlanger, S.O. and Cita, M.B. (Eds), *Nature and Origin of Cretaceous Carbon-Rich Facies*, 113–127. Academic Press; New York.
- Habib, D. 1983. Sedimentation-rate-dependent distribution of organic-matter in the North-Atlantic Jurassic–Cretaceous. *Initial Reports of the Deep Sea Drilling Project*, **76**, 781–794.†
- Habib, D., Moshkovitz, S. and Kramer, C. 1992. Dinoflagellate and calcareous nannofossil response to sea-level change in Cretaceous–Tertiary boundary sections. *Geology*, **20**, 165–168.†
- Hantar, G. 1990. North Western Desert. In: Said, R. (Ed.), *The Geology of Egypt*, 293–319. Balkema; Rotterdam.
- Harding, I. 1986. An early Cretaceous dinocyst assemblage from the Wealden of southern England. In: Batten, D.J. and Briggs, D.E.G. (Eds), *Studies in Palaeobotany and Palynology in Honour of N.F. Hughes*. *Special Papers in Palaeontology*, **35**, 95–109.
- Kerdany, M. and Cherif, O. 1990. Mesozoic. In: Said, R. (Ed.), *The Geology of Egypt*, 407–437. Balkema; Rotterdam.
- Khalaif, M. 2014. Palynological and stratigraphical studies on some subsurface Jurassic–Cretaceous rocks of North Western Desert, Egypt, 262 pp. Unpublished MSc Dissertation, Faculty of Science, Sohag University, Egypt.
- Lejzerowicz, F., Pawłowski, J., Fraissinet-Tachet, L. and Marémisse, R. 2010. Molecular evidence for widespread occurrence of Foraminifera in soils. *Environmental microbiology*, **12**, 2518–2526.
- Lister, J. and Batten, D. 1988. Stratigraphic and palaeoenvironmental distribution of Early Cretaceous dinoflagellate cysts in the Hurlands Farm Borehole, West Sussex, England. *Palaeontographica Abteilung B Paläophytologie*, **210**, 9–89.†
- Mahmoud, M.S. and Moawad, A.-R.M.M. 1999. Miospore and dinocyst biostratigraphy and palaeoecology of the Middle Cretaceous (Albian–Early Cenomanian) sequence of the Ghoroud-1X borehole, northern Western Desert, Egypt. First International Conference on the Geology of Africa, Geology Department, Assiut University, Assiut, Egypt, **1**, 1–13.
- Mahmoud, M.S., Omran, A.M. and Ataa, S.A.S. 1999. Stratigraphy of the Upper Jurassic–Lower Cretaceous sequences from three boreholes, northern Egypt: palynological evidence. *Newsletters on Stratigraphy*, **37**, 141–161.
- Mahmoud, M.S., Deaf, A.S., Tamam, M.A., and Khalaif, M.M. 2017. Palynofacies analysis and palaeoenvironmental reconstruction of the Upper Cretaceous sequence drilled by the Salam-60 well, Shushan Basin: Implications on the regional depositional environments and hydrocarbon explo-

- ration potential of north-western Egypt. *Revue de Micropaléontologie*, **60**, 449–467.
- Mahmoud, M.S., Deaf, A.S., Tamam, M.A., and Khalaf, M.M. 2019. Revised (miospores-based) stratigraphy of the Lower Cretaceous succession of the Minqar-IX well, Shushan Basin, north Western Desert, Egypt: Biozonation and correlation approach. *Journal of African Earth Sciences*, **151**, 18–35.
- Mahmoud, M.S., Khalaf, M.M., Moawad, A.-R.M.M. and Temraz, A.A. 2023. Early Cretaceous palynoflora from paleotropics of NE Africa (correlation and significance): an example from the Shushan Basin, Egypt. *Italian Journal of Geosciences*, **142**, 165–182.
- Mertens, K.N., Ribeiro, S., Bouimatarhan, I., Caner, H., Combourieu Nebout, N., Dale, B., De Vernal, A., Ellegaard, M., Filipova, M., Godhe, A., Goubert, E., Grøsfjeld, K., Holzwarth, U., Kotthoff, U., Leroy, S.A.G., Londeix, L., Marret, F., Matsuoka, K., Mudie, P.J., Naudts, L., Peña-Manjarrez, J.L., Persson, A., Popescu, S.-M., Pospelova, V., Sangiorgi, F., van der Meer, M.T.J., Vink, A., Zonneveld, K.A.F., Vercauteren, D., Vlassenbroeck, J., and Louwey, S. 2009. Process length variation in cysts of a dinoflagellate, *Lingulodinium machaerophorum*, in surface sediments: Investigating its potential as salinity proxy. *Marine Micropaleontology*, **70**, 54–69.
- Meshref, W. 1996. Cretaceous tectonics and its impact on oil exploration in northern Egypt. *Review, Geological Society of Egypt*, **2**, 199–214.
- Metwalli, F. and Pigott, J. 2005. Analysis of petroleum system criticals of the Matruh-Shushan Basin, Western Desert, Egypt. *Petroleum Geosciences*, **11**, 157–178.
- Moawad, A. 1990. Palynological studies on the subsurface, North Western Desert, Egypt. Unpublished M.Sc. Thesis, 106 pp. Faculty of Science (Qena), Assiut University (now South Valley University, Egypt).
- Mutterlose, J. and Harding, I. 1987. Phytoplankton from the anoxic sediments of the Barremian (Lower Cretaceous) of North-West Germany. *Abhandlungen der Geologischen Bundesanstalt*, **39**, 177–215.†
- Norton, P. 1967. Rock stratigraphic nomenclature of the Western Desert, Egypt. *GUPCO International Report*, **41**, 1–557.†
- Omran, A., Soliman, H. and Mahmoud, M. 1990. Early Cretaceous palynology of three boreholes from northern Western Desert (Egypt). *Review of palaeobotany and palynology*, **66**, 293–312.
- Piasecki, S. 1984. Dinoflagellate cyst stratigraphy of the Lower Cretaceous Jydegaard Formation, Bornholm, Denmark. *Bulletin of the Geological Society of Denmark*, **32**, 145–161.†
- Pittet, B. and Gorin, G. 1997. Distribution of sedimentary organic matter in a mixed carbonate-siliciclastic platform environment: Oxfordian of the Swiss Jura Mountains. *Sedimentology*, **44**, 915–937.
- Prauss, M. 2001. Sea-level changes and organic-walled phytoplankton response in a Late Albian epicontinental setting, Lower Saxony basin, NW Germany. *Palaeogeography, Palaeoclimatology, Palaeoecology*, **174**, 221–249.
- Roncaglia, L. and Kuijpers, A. 2006. Revision of the palynofacies model of Tyson (1993) based on recent high-latitude sediments from the North Atlantic. *Facies*, **52**, 19–39.
- Said, R. 1990. Cretaceous paleogeographic maps. In: Said, R. (Ed.), *The Geology of Egypt*, 439–449. Balkema; Rotterdam.
- Schrink, E. 2001. Paleoecological aspects of *Afropollis/Elaterates* peaks (Albian–Cenomanian pollen) in the Cretaceous of Northern Sudan and Egypt. In: Goodman, D. and Clarke, R. (Eds), *11th International Proceedings, Palynological Congress*, 201–210. American Association of Stratigraphers and Palynologists Foundation: Houston.
- Schrink, E. and Mahmoud, M.S. 1998. Palynology (pollen, spores and dinoflagellates) and Cretaceous stratigraphy of the Dakhla Oasis, central Egypt. *Journal of African Earth Sciences*, **26**, 167–193.
- Schrink, E. and Nesterova, E. 1993. Palynofloristic changes and Cretaceous climates in northern Gondwana (NE Africa) and southern Laurasia (Kazakhstan). In: Thorweih, U. and Schandelmeier, H. (Eds), *Geoscientific Research in Northeast Africa*, 381–390. Balkema; Rotterdam, Brookfield.
- Shalaby, M., Hakimi, M. and Abdullah, W. 2012. Geochemical characterization of solid bitumen (migrabitumen) in the Jurassic sandstone reservoir of the Tut field, Shushan Basin, northern Western Desert of Egypt. *International Journal of Coal Geology*, **100**, 26–39.
- Stancliffe, R. 1989. Microforaminiferal linings: their classification, biostratigraphy and paleoecology, with special reference to specimens from British Oxfordian sediments. *Micropaleontology*, **35**, 337–352.
- Steffen, D. and Gorin, G. 1993. Palynofacies of the Upper Ti thonian–Berriasian deep-sea carbonates in the Vocontian Trough (SE France). *Bulletin des Centres de Recherches Exploration-Production Elf-Aquitaine*, **17**, 235–247.† |
- Summerhayes, C. 1987. Organic-rich Cretaceous sediments from the North Atlantic. *Special Publications of the Geological Society, London*, **26**, 301–316.†
- Tyson, R. 1989. Late Jurassic palynofacies trends, Piper and Kimmeridge Clay Formations, UK onshore and offshore. In: Batter, D.J. and Keen, M.C. (Eds), *Northwest European Microplaeontology and Palynology*, 135–172. Ellis Horwood Publishers; Chichester.
- Tyson, R. 1993. Palynofacies analysis. In: Jenkins D.J. (Ed.), *Applied Micropalaeontology*, 153–191. Kluwer Academic Publishers; Dordrecht, The Netherlands.
- Tyson, R. 1995. Sedimentary organic matter: organic facies and palynofacies, 615 pp. Chapman and Hall; London.
- Uwins, P. and Batten, D. 1988. Early to mid-Cretaceous palynology of northeast Libya. In: El-Arnauti, A., Owens, B. and Thusu, B. (Eds), *Subsurface palynostratigraphy of*

- northeast Libya, 215–257. Garyounis University Publications; Benghazi.
- Vail, P., Mitchum, J. and Thompson, S. 1977. Seismic stratigraphy and global changes of sea level, Part 4: Global cycles of relative changes of sea level. *Seismic Stratigraphy: Application to Hydrocarbon Exploration. American Association of Petroleum Geologists Memoirs*, **26**, 83–97.
- Vallejo, C., Hochuli, P., Winkler, W. and Von Salis, K. 2002. Palynological and sequence stratigraphic analysis of the Napo Group in the Pungarayacu 30 well, Sub-Andean Zone, Ecuador. *Cretaceous Research*, **23**, 845–859.
- Van der Meer, D.G., Scotese, C.R., Mills, B.J., Sluijs, A., van den Berg van Saparoea, A.-P. and van De Weg, R.M.B. 2022. Long-term Phanerozoic global mean sea level: Insights from strontium isotope variations and estimates of continental glaciation. *Gondwana Research*, **111**, 103–121.
- Zonneveld, K.A.F., Marret, F., Versteegh, G.J.M., Bogus, K., Bonnet, S., Bouimetarhan, I., Crouch, E., de Vernal, A., Elshanawany, R., Edwards, L., Esper O., Forke, S., Grøsfjeld, K., Henry, M., Holzwarth, U., Kielt, J.-F., Kim, S.-Y., Ladouceur, S., Ledu, D., Chen, L., Limoges, A., Londeix, L., Lu, S.-H., Mahmoud, M.S., Marino, G., Matsouka, K., Matthiessen, J., Mildenhall, D.C., Mudie, P., Neil, H.L., Pospelova, V., Qi, Y., Radi, T., Richerol, T., Rochon, A., Sangiorgi, F., Solignac, S., Turon, J.-L., Verleye, T., Wang, Y., Wang, Z. and Young, M. 2013. Atlas of modern dinoflagellate cyst distribution based on 2405 datapoints. *Review of Palaeobotany and Palynology*, **191**, 1–197.

Manuscript submitted: 30th January 2024

Revised version accepted: 15th May 2024

Appendix 1. Palynomorph semi-quantitative percentage frequency distribution chart of spores, pollen, dinoflagellate cysts and microforaminiferal test linings in the investigated succession of the Shushan-1X well. Palynomorph distribution data presented by Mahmoud et al. (2023) are used herein for paleoenvironmental reconstruction.

Sample no.	Depth (ft)	Depth (m)	Stage/Substage	Formation	Spores
132	5510	1679			
130	5610	1710			
125	5960	1817			
117	6560	1999			
115	6670	2033			
113	6790	2070			
112	6840	2085			
110	6940	2115			
108	7050	2149			
104	7290	2222			
101	7570	2307			
98	7770	2368			
96	7890	2405			
95	7930	2417			
92	8220	2505			
89	8670	2643			
84	9230	2813			
77	9960	3036			
70	10300	3139			
68	10410	3173			
65	10570	3222			
61	10730	3271			
60	10770	3283			
58	10850	3307			
57	10890	3319			
55	11030	3362			
53	11120	3389			
45	11490	3502			
40	11740	3578			
37	11780	3591			
33	11860	3615			
29	11910	3630			
25	11960	3645			
21	12010	3661			
17	12060	3676			
12	12170	3709			
10	12210	3722			
5	12300	3749			
3	12340	3761			
1	12380	3773			
			Lower-Middle Cenomanian		
			Upper Albian		
			Middle Albian		
			Upper Aptian		
			Lower Aptian		
			Barremian		
			Upper Barremian		
			Lower Barremian		
			Hauterivian		
			Lower Hauterivian		
			Upper Valanginian		
			Lower Valanginian		
			Alam El-Bieb		
			Alamein		
			Dahab		
			Kharita		
			Barremian		
			Formation		
			Spores		
			1-Triplanospores sp.		
			2-Deltodiscospores spp.		
			3-Diclopylylithites narsisi		
			4-Cicanicosisporites sp.		
			5-Diclopylylithites narsisi		
			6-Crybeliosporites pannicum		
			7-Deltodiscospores oralis		
			8-Todisporites minor		
			9-Deltodiscospores australis		
			10-Concavissimospites sp.		
			11-Venustosporites spp.		
			12-Chlobutisporata jurensis		
			13-Antillinasporites scandicus		
			14-Matisonspores sp.		
			15-Murosphaera florida		
			16-Citacrinisporites sinuosus		
			17-Concavissimospites punctatus		
			18-Deltodiscospora hawaii		
			19-Gleichenioides sp.		
			20-Kyrtomisporis sp.		
			21-Baimesporites holodictyus		
			22-Aequitradisites nomissii		
			23-Biretisporites potoniae		
			24-Echinula spores		
			25-Concavissimospites varivenatus		
			26-Imparacisporula spinulosus		
			27-Citacrinisporites cf. dongensis		
			28-Aequitradisites spinulosus		
			29-Phlosisporites trichopapillatus		

	Gymnosperm pollen					
30-Araucariaceites australis						
31-Casuarinacées classées des						
32-Ephédracées sp.						
33-Cycadacées sp.						
34-Inaperturopollenites sp.						
35-Callialaspites brasiliensis						
36-Equisetopollenites sp.						
37-Callialaspites dampieri						
38-Classopollenites sp.						
39-Taxodiaceopollenites sp.						
40-Callialaspites tributatus						
41-Baumholderites limbanus						
42-Classopollenites sp.						
43-Taxacites sahariensis						
44-Dicroidiopolis ethicus						
45-Spheneropollenites sp.						
	Elatostemoid pollen					
46-Ellipteropollenites kleissii						
47-Elleropollenites castelainii						
48-Elleropollenites africanaensis						
	Angiosperm pollen					
49-Alycopis jardinius						
50-Reinmucopollenites variiflavus						
51-Tricolites spp.						
52-2Alycopis kehrmannensis						
53-Alycopis spp.						
54-Foerstrocpollenites gérardoreculanus						
55-Tucanopollenites annulatus						
56-Stellatopollenites dejazi						
57-cl. Alycopis sp.						
58-Alycopis aff. jardinius						
59-Reinmucopollenites ghazalzaii						
60-Reinmucopollenites paeniyi						
61-Eucoccolites spp.						
62-Reinmucopollenites sp.						
63-Dicranopollenites ghazalzaii						
64-Alycopis operculatus						
65-Stellatopollenites spp.						
66-Alycopis zonatus						
67-Monocotopollenites sp.						

Dinoflagellate cysts		Microfilarial test linings		Total pollen		Total palynomorphs	
68-Sulfolisphaera senegalensis							
69-Sulfolisphaera scabula							
70-Coconiera oceanica							
71-Sulfolisphaera sp.							
72-Florenina mazellii	2.2	0.7	1.5	0.7	1.5	8.2	10.4
73-Escherschaeferia sp.	0.9	1.4	0.9	0.5		2.7	6.3
74-Spiniferites sp.	0.9	1.3	3.4	3.8		1.7	8.5
75-Sulfolisphaera terra	2.5	4.6	2.1	2.9	2.1	17.8	19.7
76-Coconiera alienii	1.7	0.8	1.7	1.3	1.3	4.2	10.0
77-Oligosphaeridium complex	0.5	1.6	2.6	0.5		2.1	4.9
78-Apedinum sp.	4.5	10.1	3.4	3.9	1.7	2.1	42.9
79-Oligosphaeridium alberense	0.9	0.9	2.8	1.9		2.0	34.2
80-Florenina beran	0.4	1.0	0.5			2.2	22.9
81-Sulfolisphaera perlucida	1.0	1.0	1.0			2.2	100.0
82-Aptea polymorpha	0.4	1.0	1.0			2.6	9.7
83-Oligosphaeridium diluculum						3.7	10.0
84-Pseudobertinium retusum						2.7	10.0
85-Palaeoperidinium creaceum						1.7	10.0
86-cl. Circulodinium distinctum						4.2	10.0
87-Pseudobertinium secundigenum						2.1	10.0
88-Florenina cookeanae						2.6	10.0
89-Pseudobertinium anaphytissum						3.9	10.0
90-Odonochitina opercularia						2.8	10.0
91-Oxydinephelium vanoporthorum						0.8	10.0
92-Cyrtoperidinium sp.						1.5	10.0
93-Chonetekidinium edwardsi						1.2	10.0
94-Oligosphaeridium poculum						1.4	10.0
95-Circulodinium distinctum						0.6	10.0
96-Peredinia ceratophora						0.5	100.0
97-Mutileongia sp.						3.0	3.5
98-Cytoperoxydinium orthoceras						3.1	0.0
Unidentified dinoflagellate cysts						0.9	0.0
Dinoflagellate cysts						31.8	58.5
Micoforaminal test linings						5.5	9.7
Total spores						29.1	18.7
Total pollen						100.0	100.0
Total palynomorphs							

Appendix 2. List of the total recovery of palynomorphs in the Shushan-1X well.

Appendix 3. List of palynomorph groups used in the construction of the SMP ternary diagram for the Shushan-1X well, presented in Text-fig. 8A.

Sample no.	Formation	Pollen	Micoplankton	Spores	Total palynomorphs	Pollen %	Micoplankton %	Spores %	Total palynomorphs %
132	Bahariya	39	25	70	134	29.1	18.7	52.2	100.0
130		44	23	154	221	19.9	10.4	69.7	100.0
125		104	46	84	234	44.4	19.7	35.9	100.0
117		82	55	103	240	34.2	22.9	42.9	100.0
115		138	23	75	236	58.5	9.7	31.8	100.0
113		124	20	47	191	64.9	10.5	24.6	100.0
112		69	65	45	179	38.5	36.3	25.1	100.0
110		110	30	71	211	52.1	14.2	33.6	100.0
108	Kharita	87	21	132	240	36.3	8.8	55.0	100.0
104		100	15	81	196	51.0	7.7	41.3	100.0
101		88	43	118	249	35.3	17.3	47.4	100.0
98		66	16	126	208	31.7	7.7	60.6	100.0
96		80	5	86	171	46.8	2.9	50.3	100.0
95		105	9	88	202	52.0	4.5	43.6	100.0
92		48	13	140	201	23.9	6.5	69.7	100.0
89		31	6	158	195	15.9	3.1	81.0	100.0
84	Dahab	16	4	189	209	7.7	1.9	90.4	100.0
77		111	75	42	228	48.7	32.9	18.4	100.0
70	Alamein	55	3	169	227	24.2	1.3	74.4	100.0
68		108	10	67	185	58.4	5.4	36.2	100.0
65		46	9	171	226	20.4	4.0	75.7	100.0
61		91	3	156	250	36.4	1.2	62.4	100.0
60		107	11	72	190	56.3	5.8	37.9	100.0
58		93	9	155	257	36.2	3.5	60.3	100.0
57		71	58	119	248	28.6	23.4	48.0	100.0
55		96	16	106	218	44.0	7.3	48.6	100.0
53		97	14	108	219	44.3	6.4	49.3	100.0
45		78	15	120	213	36.6	7.0	56.3	100.0
40	Alam El-Bueib	104	9	125	238	43.7	3.8	52.5	100.0
37		106	26	87	219	48.4	11.9	39.7	100.0
33		60	16	104	180	33.3	8.9	57.8	100.0
29		108	10	82	200	54.0	5.0	41.0	100.0
25		97	18	126	241	40.2	7.5	52.3	100.0
21		139	8	73	220	63.2	3.6	33.2	100.0
17		95	7	86	188	50.5	3.7	45.7	100.0
12		65	11	113	189	34.4	5.8	59.8	100.0
10		82	5	109	196	41.8	2.6	55.6	100.0
5		53	5	87	145	36.6	3.4	60.0	100.0
3		62	6	128	196	31.6	3.1	65.3	100.0
1		62	9	95	166	37.3	5.4	57.2	100.0

Appendix 4. List of different palynofacies categories used in the construction of the APP ternary plot for the Shushan-1X well, presented in Text-fig. 8B.

Sample no.	Formation	Depth (ft)	Depth (m)	Palynomorphs	Phytoclasts	AOM	Total Palynofacies	Palynomorphs %	Phytoclasts %	AOM %	Total Palynofacies %
135	Banatia	5340	1628	1	33	466	500	0.0	6.6	93.2	99.8
134		5390	1643	16	310	185	511	3.1	60.7	36.2	100.0
133		5420	1652	3	115	385	503	0.6	22.9	76.5	100.0
132		5510	1679	40	355	115	510	7.8	69.6	22.5	100.0
131		5580	1701	11	233	270	514	2.1	45.3	52.5	100.0
130		5610	1710	21	270	220	511	4.1	52.8	43.1	100.0
129		5660	1725	6	195	300	501	1.2	38.9	59.9	100.0
128		5760	1756	0	45	455	500	0.0	9.0	91.0	100.0
127		5800	1768	4	236	273	513	0.8	46.0	53.2	100.0
126		5840	1780	7	277	224	508	1.4	54.5	44.1	100.0
125		5960	1817	12	250	240	502	2.4	49.8	47.8	100.0
124		6010	1832	4	230	275	509	0.8	45.2	54.0	100.0
123		6160	1878	5	136	360	501	1.0	27.1	71.9	100.0
122		6260	1908	6	66	440	506	0.0	13.0	87.0	100.0
121		6290	1917	1	20	480	501	0.2	4.0	95.8	100.0
120		6350	1935	2	162	340	504	0.4	32.1	67.5	100.0
119	Kharta	6400	1951	3	36	468	507	0.6	7.1	92.3	100.0
118		6460	1969	3	76	430	509	0.6	14.9	84.5	100.0
117		6560	1999	8	101	394	503	1.6	20.1	78.3	100.0
116		6610	2015	12	147	342	501	2.4	29.3	68.3	100.0
115		6670	2033	34	231	241	506	6.7	45.7	47.6	100.0
114		6710	2045	25	263	220	508	4.9	51.8	43.3	100.0
113		6790	2070	15	296	202	513	2.9	57.7	39.4	100.0
112		6840	2085	12	150	350	512	2.3	29.3	68.4	100.0
111		6900	2103	20	231	260	511	3.9	45.2	50.9	100.0
110		6940	2115	16	257	241	514	3.1	50.0	46.9	100.0
109		7000	2134	12	212	276	500	2.4	42.4	55.2	100.0
108		7050	2149	29	159	316	504	5.8	31.5	62.7	100.0
107		7110	2167	28	266	214	508	5.5	52.4	42.1	100.0
106		7180	2188	10	186	307	503	2.0	37.0	61.0	100.0
105		7230	2204	11	223	270	504	2.2	44.2	53.6	100.0
104		7290	2222	8	208	295	511	1.6	40.7	57.7	100.0
103		7400	2256	10	316	180	506	2.0	62.5	35.6	100.0
102		7450	2271	8	403	96	507	1.6	79.5	18.9	100.0
101		7570	2307	16	295	200	511	3.1	57.7	39.1	100.0
100		7610	2320	7	336	167	510	1.4	65.9	32.7	100.0
99		7670	2338	26	306	174	506	5.1	60.5	34.4	100.0
98		7770	2368	23	322	164	509	4.5	63.3	32.2	100.0
97		7810	2380	16	293	200	509	3.1	57.6	39.3	100.0
96		7890	2405	10	242	255	507	2.0	47.7	50.3	100.0
95		7930	2417	32	395	75	502	6.4	78.7	14.9	100.0
94		8070	2460	29	314	170	513	5.7	61.2	33.1	100.0
93		8160	2487	17	280	204	501	3.4	55.9	40.7	100.0
92		8220	2505	34	358	108	500	6.8	71.6	21.6	100.0
91		8280	2524	9	232	259	500	1.8	46.4	51.8	100.0

cont.

cont.

Formation	Kharta	Dahab	Alamein	Alam El-Bieb
90	8330	2539		
89	8670	2643		
88	8710	2655		
87	8950	2728		
86	9120	2780		
85	9180	2798		
84	9230	2813		
83	9270	2825		
82	9550	2911		
81	9600	2926		
80	9650	2941		
79	9700	2957		
78	9910	3021		
77	9960	3036		
76	10000	3048		
75	10030	3057		
74	10080	3072		
73	10180	3103		
72	10210	3112		
71	10250	3124		
70	10300	3139		
69	10360	3158		
68	10410	3173		
67	10460	3188		
66	10520	3206		
65	10570	3222		
64	10620	3237		
63	10660	3249		
62	10700	3261		
61	10730	3271		
60	10770	3283		
59	10820	3298		
58	10850	3307		
57	10890	3319		
56	10980	3347		
55	11030	3362		
54	11070	3374		
53	11120	3389		
52	11170	3405		
51	11240	3426		
50	11300	3444		
49	11340	3456		
48	11370	3466		
47	11410	3478		
46	11450	3490		

Formation	Kharta	Dahab	Alamein	Alam El-Bieb
45	11490	3502		
44	11530	3514		
43	11570	3527		
42	11650	3551		
41	11690	3563		
40	11740	3578		
39	11760	3584		
38	11770	3587		
37	11780	3591		
36	11800	3597		
35	11810	3600		
34	11850	3612		
33	11860	3615		
32	11880	3621		
31	11890	3624		
30	11900	3627		
29	11910	3630		
28	11920	3633		
27	11930	3636		
26	11950	3642		
25	11960	3645		
24	11980	3652		
23	11990	3655		
22	12000	3658		
21	12010	3661		
20	12030	3667		
19	12040	3670		
18	12050	3673		
17	12060	3676		
16	12090	3685		
15	12110	3691		
14	12120	3694		
13	12150	3703		
12	12170	3709		
11	12200	3719		
10	12210	3722		
9	12230	3728		
8	12260	3737		
7	12280	3743		
6	12290	3746		
5	12300	3749		
4	12320	3755		
3	12340	3761		
2	12360	3767		
1	12380	3773		